Cellular/Molecular

Uropathic Observations in Mice Expressing a Constitutively Active Point Mutation in the 5-HT$_{3A}$ Receptor Subunit

Anindya Bhattacharya,[1] Hong Dang,[2] Quan-Ming Zhu,[1] Birthe Schnegelsberg,[1] Nora Rozengurt,[3] Gary Cain,[1] Rachelle Prantil,[4] David A. Vorp,[4] Nicholas Guy,[5] David Julius,[5] Anthony P. D. W. Ford,[1] Henry A. Lester,[2] and Debra A. Cockayne[1]

[1]Roche Pharmaceuticals, Palo Alto, California 94304, [2]Caltech, Pasadena, California 91125, [3]Department of Pathology and Laboratory Medicine, University of California Los Angeles, Los Angeles, California 90095, [4]Departments of Surgery and Bioengineering, University of Pittsburgh, Pittsburgh, Pennsylvania 15213, and [5]Department of Cell and Molecular Pharmacology, University of California San Francisco, San Francisco, California 94143

Mutant mice with a hypersensitive serotonin (5-HT)$_{3A}$ receptor were generated through targeted exon replacement. A valine to serine mutation (V13′S) in the channel-lining M2 domain of the 5-HT$_{3A}$ receptor subunit rendered the 5-HT$_3$ receptor ~70-fold more sensitive to serotonin and produced constitutive activity when combined with the 5-HT$_{3B}$ subunit. Mice homozygous for the mutant allele (5-HT$_{3A}$$^{vs/vs}$) had decreased levels of 5-HT$_{3A}$ mRNA. Measurements on sympathetic ganglion cells in these mice showed that whole-cell serotonin responses were reduced, and that the remaining 5-HT$_3$ receptors were hypersensitive. Male 5-HT$_{3A}$$^{vs/vs}$ mice died at 2–3 months of age, and heterozygous (5-HT$_{3A}$$^{vs/+}$) males and homozygous mutant females died at 4–6 months of age from an obstructive uropathy. Both male and female 5-HT$_{3A}$ mutant mice had urinary bladder mucosal and smooth muscle hyperplasia and hypertrophy, whereas male mutant mice had additional prostatic smooth muscle and urethral hyperplasia. 5-HT$_{3A}$ mutant mice had marked voiding dysfunction characterized by a loss of micturition contractions with overflow incontinence. Detrusor strips from 5-HT$_{3A}$$^{vs/vs}$ mice failed to contract to neurogenic stimulation, despite overall normal responses to a cholinergic agonist, suggestive of altered neuronal signaling in mutant mouse bladders. Consistent with this hypothesis, decreased nerve fiber immunoreactivity was observed in the urinary bladders of 5-HT$_{3A}$$^{vs/vs}$ compared with 5-HT$_{3A}$ wild-type (5-HT$_{3A}$$^{+/+}$) mice. These data suggest that persistent activation of the hypersensitive and constitutively active 5-HT$_{3A}$ receptor *in vivo* may lead to excitotoxic neuronal cell death and functional changes in the urinary bladder, resulting in bladder hyperdistension, urinary retention, and overflow incontinence.

Key words: 5-HT$_3$; mouse; knock-in mutation; bladder; hypertrophy; afferent innervation

Introduction

The serotonin (5-HT) 3 receptor is unique among the 5-HT receptor subtypes because it belongs to the family of excitatory ligand-gated ion channels. Pentamers of 5-HT$_{3A}$ subunits can form the channel pore, where each subunit has four transmembrane domains, the second (M2) of which lines the ion channel (van Hooft and Yakel, 2003). 5-HT$_3$ receptors can exist functionally as either homopentameric channels of the 5-HT$_{3A}$ subunit or as heteromers with the recently cloned auxiliary 5-HT$_{3B}$ subunit (Davies et al., 1999). However, because the 5-HT$_{3B}$ subunit alone cannot produce functional receptors, the 5-HT$_{3A}$ subunit is an essential component of all serotonin-gated ion channels (Dubin et al., 1999; Dang et al., 2000).

5-HT$_3$ receptors are expressed in both the peripheral and CNS and have been implicated in CNS functions such as cognition,

anxiety and emesis, as well as sympathetic, parasympathetic, and sensory functions in the peripheral nervous system (PNS) (Tecott et al., 1993; Jackson and Yakel, 1995; Johnson and Heinemann, 1995; Morales and Wang, 2002). 5-HT$_3$ receptors are important in nociceptive processing (Alhaider et al., 1991; Eide and Hole, 1993; Zeitz et al., 2002), consistent with expression on primary sensory afferents in the dorsal root ganglion (DRG) and on neurons in the dorsal horn of the spinal cord (Hamon et al., 1989; Kidd et al., 1993, Tecott et al., 1993; Kia et al., 1995; Morales and Wang, 2002; Zeitz et al., 2002). 5-HT$_3$ receptors on vagal sensory afferents modulate visceral afferent and efferent information in the gastrointestinal tract and cardiovascular system (Leslie et al., 1990; Merahi et al., 1992; Veelken et al., 1993; Sevoz-Couche et al., 2003). In the enteric nervous system, 5-HT$_3$ receptors also regulate gut motility and peristalsis (Galligan, 2002). Within the lower urinary tract, presynaptic 5-HT$_3$ receptors have been implicated in parasympathetic transmission to the urinary bladder through neuronal acetylcholine (ACh) release and smooth muscle contraction (Chen, 1990; Barras et al., 1996).

Various mutations in the M2 domain of the 5-HT$_{3A}$, nicotinic ACh (nACh), GABA$_A$, and glycine receptors have been shown to produce hypersensitivity to agonist stimulation. Some of these mutations occur naturally and are pathologic (Lester and Kar-

schin, 2000), and knock-in mice carrying hypersensitive nicotinic receptor mutations have yielded (patho)physiological insights into nACh receptor function (Lester et al., 2003). To date, there are no known diseases or animal models linked to point mutations of 5-HT$_{3A}$ receptors. A valine to serine mutation in the M2 domain of the 5-HT$_{3A}$ receptor subunit (V13′S) was previously shown to produce a homomeric receptor ~70-fold more sensitive to 5-HT than the wild-type (WT) receptor when expressed in oocytes (Dang et al., 2000). The purpose of the present study was to further characterize the hypersensitive V13′S mutation *in vitro* and to evaluate the V13′S mutation as a gain of function alteration in gene knock-in mice.

Coexpression of the mutant 5-HT$_{3A}$ subunit with the wild-type 5-HT$_{3B}$ subunit resulted in a 5-HT$_3$ receptor that was constitutively active in addition to showing hypersensitivity to 5-HT. Introduction of the V13′S mutation into mice by targeted exon replacement resulted in expression of 5-HT$_{3A}$$^{vs/vs}$ receptors that were similarly hypersensitive and constitutively active. Unexpectedly, 5-HT$_{3A}$$^{vs/vs}$ mice died prematurely from complications related to bladder overactivity, chronic urinary retention, and urinary tract outlet obstruction. Additional characterization of the morphologic, pharmacologic, and cystometric changes in the urinary bladder and urethral outlet tissues of 5-HT$_{3A}$ mutant mice showed that many of these changes are characteristic of urinary bladder outlet obstruction (BOO), as seen in patients with benign prostatic hyperplasia (BPH) or neuropathic lesions (Turner and Brading, 1997). These data may reflect an important role of 5-HT$_3$ receptors in lower urinary tract (patho)physiology.

Materials and Methods

Targeted exon replacement of the 5-HT$_{3A}$ receptor. A 6 kb genomic DNA fragment was cloned from a mouse 129Sv/J genomic library (Stratagene, La Jolla, CA) that contained exons 6–9 of the mouse 5-HT$_{3A}$ gene. This fragment was cloned into the pGEM5-Zf(+) vector (Promega, Madison, WI), and the M2 channel domain encoded by exon 7 was mutated to change the Val13′ GTC codon to TCA encoding serine (V13′S). Mutagenesis was performed with the Quick-Change mutagenesis kit (Stratagene) using the following oligonucleotide and its complement: 5′-CTT CTG GGA TAC TCA *TCA* (Ser) TTC CTC ATC ATC GTG-3′. This mutation eliminated a native *Dde*I site (CTNAG) in exon 7, which was later used for screening the mutation. The targeting vector was generated by introducing a *Lox*P-flanked neomycin resistance cassette (Neo), driven by the phosphoglycerate kinase (PGK) promoter, into a *Swa*I site in intron 5 and a PGK-thymidine kinase (TK) cassette into the 3′ end of the genomic clone. A *Not*I linearized targeting vector was electroporated into 129Sv/J-derived CJ7 embryonic stem (ES) cells, and homologous recombinant ES clones were double selected in the presence of 180 μg/ml active G418 (Sigma, St. Louis, MO) and 0.2 μM 2′-fluoro-2′-deoxy-1β-D-arabino-furanosyl-5-iodo-uracil (FIAU; Sigma). G418 and FIAU resistant ES clones were identified by PCR using a 5′-flanking primer (5F) upstream of the targeting vector sequence (5′-AGC TGC CTT CCT CTG GAT GCC TAG AGG TCC-3′) and a 3′ primer (NI) internal to the Neo cassette (5′-GAT CAG CAG CCT CTG TTC CAC ATA CAC TTC ATT CTC-3′). Recombinant ES clones were confirmed by *Eco*RI Southern blot analysis using both 5′- and 3′-flanking region probes. The 5-HT$_{3A}$ wild-type allele contained a 10 kb *Eco*RI fragment detected by both the 5′- and 3′-probes. Incorporation of the Neo cassette introduced an *Eco*RI site into the targeted allele, resulting in detection of a 5.5 kb fragment by the 5′-probe and a 7 kb fragment by the 3′-probe. Five of 672 ES clones screened were confirmed as homologous recombinants. The integrity of the V13′S mutation was demonstrated with a PCR assay that amplified a 390 bp amplicon across exons 7–8 using primers VS1 (5′-CCG GAG GCC TTT ATT CTA CGC AGT CAG CCT C-3′) and VS2 (5′-CTG GCC GCT GTA GGT CCT GCT TAT GCA CC-3′). To detect the mutation, the PCR product was further digested with *Dde*I to generate amplicons of ~210 and ~140 bp for the mutant and wild-type alleles, respectively

(mutation deleted 1 of 3 *Dde*I sites in the fragment). The PCR amplicon was further sequenced with primer VS3 (5′-CAG TAT CTT CCT CAT GGT CGT GG-3′). This PCR assay was used as the primary genotyping assay for 5-HT$_{3A}$ knock-in mice.

ES clones were injected into C57BL/6J embryos, and germline transmission was established by mating chimeras to the C57BL/6J strain. To minimize the possible effect of the Neo cassette on the expression of the mutant allele, the Neo gene was deleted from the targeted locus by mating 5-HT$_{3A}$ mutant mice with a transgenic mouse line expressing Cre recombinase under the control of a cytomegalovirus promoter-enhancer (DBA/2tg-2.6; provided as a gift from D. Anderson, Caltech, Pasadena, CA) (Zinyk et al., 1998). Cre-mediated recombination at the two *Lox*P sites flanking the Neo gene resulted in a single *Lox*P sequence of 34 bp remaining at the insertion site. Neo-deleted clones were identified by Southern blot and DNA sequence analysis as described above for ES clone screening, as well as by PCR across the Neo deletion site. This PCR assay used primers ND1 (5′-AAC TCT AAC AAA GAA ACA TAG AAG GTT GTT TGG AAG G-3′) and ND2 (5′-CAA TCA TAG AAC CTT CGA GCA TAG AAG GTG G-3′) and amplified a 334 bp fragment containing the single *Lox*P site. All mice used for studies were derived from subsequently established heterozygous (5-HT$_{3A}$$^{vs/+}$) breeding pairs maintained on a mixed genetic background of 129Sv/J × C57BL/6J × DBA/2. All animal use procedures were overseen and approved by the Roche Palo Alto Institutional Animal Care and Use Committee or the Caltech Institutional Animal Care and Use Committee.

Reverse transcriptase PCR analysis of 5-HT$_{3A}$ transcripts in 5-HT$_{3A}$ wild-type and mutant mice. Total superior cervical ganglion (SCG) RNA was isolated using the RNAzol B reagent (Tel-Test,, Friendswood, TX) according to supplier specifications. RNA samples were diluted 1:100, and reverse transcriptase (RT)-PCR was performed using 1 μl of serial dilutions of RNA as template in a 25 μl reaction using the Thermoscript One-Step RT-PCR kit (Invitrogen, Rockville, MD). The primers used for amplification of the 5-HT$_{3A}$ receptor were VS1 and VS2 (described above), and the primers used for amplification of the α7 nACh receptor internal control were 7-1 (5′-GAT CAC TAT TTG CAG TGG AAC ATG TCT GAG TAC C-3′) and 7-2 (5′-CAT GAT CTC AGC CAC AAG CAG CAT GAA G-3′). Both sets of primers were amplified simultaneously in the PCR to generate amplicons of 300 and 700 bp for the 5-HT$_{3A}$ and α7 nACh receptors, respectively.

Quantitation of mRNA derived from mutant or wild-type alleles was estimated from the relative representation of the mutant and wild-type sequences obtained by sequencing the RT-PCR products derived from 5-HT$_{3A}$$^{vs/+}$ mice. This approach is based on the premise that although automatic DNA sequencing signals are highly variable at individual nucleotide positions, these signals retain their relative sizes within a given stretch of sequence when compared among DNA samples sequenced under identical conditions. In comparing the relative signals from the mutation to nearby constant nucleotides between wild-type and mutant sequences, one can estimate the relative amount of mutant versus wild-type mRNA in heterozygous mice. After sequencing of the RT-PCR products from 5-HT$_{3A}$$^{+/+}$, 5-HT$_{3A}$$^{vs/+}$, and 5-HT$_{3A}$$^{vs/vs}$ mice using primer VS3, the area under the wild-type and mutant peaks was normalized to the 3T and 1A nucleotide positions (numbered with respect to the wild-type V13′ codon GTC). The peak area ratios 1G/-3T and 1G/-1A in 5-HT$_{3A}$$^{+/+}$ RT-PCR products defined pure wild-type sequence, and the peak area ratios of (1T or 2C or 3A)/(-3T or -1A) in the 5-HT$_{3A}$$^{vs/vs}$ RT-PCR products defined pure mutant sequence. The normalized signal from 1G (GTC valine codon) was used to estimate the amount of wild-type sequence (the 5-HT$_{3A}$$^{+/+}$ sample was defined as 100%). Similarly, the normalized signals from 1T, 2C, and 3A (TCA serine codon) were used to estimate the amount of mutant sequence (the 5-HT$_{3A}$$^{vs/vs}$ sample was defined as 100%). Using this approach, average estimates were made of the amount of mutant and wild-type mRNA expressed in 5-HT$_{3A}$$^{vs/+}$ mice.

Xenopus *oocyte electrophysiology.* As described previously (Dang et al., 2000), cDNA clones for the mouse 5-HT$_{3A}$ subunit (Maricq et al., 1991) and for the human 5-HT$_{3B}$ cDNA (Davies et al., 1999) were subcloned into the oocyte expression vector plasmid pAMV (Nowak et al., 1995). Mutations in the cDNA were made using the Quick-Change mutagenesis

kit (Stratagene). Plasmids were linearized with *Not*I and used as template to produce mRNA using the T7 mMESSAGE mMACHINE kit (Ambion, Austin, TX). Stage V-VI *Xenopus* oocytes were harvested and injected with 50 nl of cRNA per oocyte (~0.5 ng/oocyte). The ratio between the 5-HT$_{3A}$ and the 5-HT$_{3B}$ mRNA was 1:1. Two-electrode voltage-clamp recordings were performed 24–36 hr after injection using a GeneClamp500 circuit, a Digidata 1200 digitizer, and pClamp software (Axon Instruments, Union City, CA). The recording solution contained (in mM): 96 NaCl, 2 KCl, 2 MgCl$_2$, 5 HEPES, pH 7.4 (ND 96). Whole-cell current responses to various drug concentrations at indicated holding potentials (typically −60 mV) were fitted to the Hill equation, $I/I_{max} = 1/[1 + (EC_{50}/[A])^n]$, where I is agonist-induced current at concentration $[A]$, I_{max} is the maximum current, EC_{50} is the concentration inducing half-maximum response, and n is the Hill coefficient.

Primary cell culture and electrophysiology. SCG neurons were dissected from 1- to 3-d-old mice and digested in Ca^{2+}, Mg^{2+}-free Hank's saline solution containing 0.25% trypsin for 10 min. Cell suspensions were washed and gently triturated, followed by plating onto culture dishes precoated with polyornithine and laminin in MEM supplemented with 2% B-27 (Invitrogen), 0.5 mM GlutaMax I (Invitrogen), and 10 ng/ml nerve growth factor (Sigma). Neurons were studied by patch-clamp recording after 3–10 d in culture. Whole-cell patch-clamp recordings were performed at room temperature with the following external solution (in mM): 140 NaCl, 4 KCl, 2 CaCl$_2$, 2 MgCl$_2$, 10 HEPES, pH 7.4. Recording electrodes had the following intracellular solution (in mM): 140 CsCl, 2 MgCl$_2$, 1.1 EGTA, 0.1 CaCl$_2$, 10 HEPES, pH 7.3. For recording 5-HT-gated currents, cells were held at −80 mV. All patched cells were verified for their neuronal properties by the presence of voltage-gated sodium currents. Recordings were performed with an Axopatch 2A amplifier, Digidata 1200 digitizers, an IBM compatible personal computer, and pClamp6 or pClamp8 software (Axon Instruments) with standard patch-clamp protocols. Drugs were delivered through a multi-barrel manifold with an inner diameter of 250 μm.

Histopathology and immunohistochemistry. Complete full-body necropsies were performed on adult 5-HT$_{3A}$$^{+/+}$ and 5-HT$_{3A}$$^{vs/vs}$ mice, and histopathology was performed on 40 postmortem tissues covering all major organ systems. After removal, tissues were immersed in 4% buffered formalin and embedded in paraffin wax. Four micrometer sections were cut and stained with hematoxylin and eosin (H and E). For whole-mount immunohistochemical staining of the bladder urothelium (Gabella and Davis, 1998), whole bladders were isolated from euthanized animals. Isolated bladders were opened by cutting the tissue from the base to the dome, and the tissue was stretched by pinning it down with small dissection pins (Watkins, Doncaster, UK) onto balsa wood while keeping the tissue wet with PBS. The tissue was fixed by immersing the pinned tissue in 10% buffered formalin at 4°C for 4 hr. After fixation, the urothelial layer was carefully separated from the underlying smooth muscle layer under a dissecting microscope. For urothelial whole-mount staining, the tissue was blocked with PBS containing 20% normal goat serum and 0.2% Triton X-100 for 2 hr at room temperature. The first antibody was applied in PBS containing 5% normal goat serum, 0.2% Triton X-100 overnight at 4°C. A rat Substance P antibody (Accurate Chemicals, Westbury, NY) was used at a 1:500 dilution, and a rabbit protein gene product (PGP) 9.5 antibody (Ultraclone, Isle of Wight, UK) was used at a 1:6000 dilution. The tissue was washed four times for 15 min at room temperature in PBS containing 0.1% BSA and 0.1% Triton X-100. A secondary cytochrome-3 antibody (Jackson ImmunoResearch, West Grove, PA) was applied at a concentration of 1:500 for Substance P staining and 1:300 for PGP 9.5 staining for 4 hr at room temperature in the same solution. The tissue was washed three times for 10 min in PBS and mounted with Mounting medium (Polysciences, Warrington, PA). Immunostaining was analyzed with a Nikon (Tokyo, Japan) Microphot SA fluorescence microscope, and the observer was blinded to the identity of the samples when scoring immunoreactivity.

Mouse cystometry. Mice were anesthetized with isoflurane and cystometry was conducted as described previously (Cockayne et al., 2000). Briefly, the bladder was exposed through a midline abdominal incision. A saline-filled PE-10 cannula with an enlarged tip was inserted into the dome of the bladder and secured to the bladder with 5-0 Tevdek suture.

The cannula was tunneled subcutaneously to the back, exteriorized, tied off, and secured to the skin with 4-0 silk. The muscle layer was closed with 4-0 silk, the skin incision was closed, and the exteriorized part of the catheter was placed into the subcutaneous space. Mice were returned to normal caging for 7 d of recovery. For conscious cystometry, each mouse was placed in a restraint box within a metabolic cage. The bladder cannula was exteriorized and connected to a pressure transducer and infusion pump via a three-way connector. Normal saline was infused into the bladder at a constant rate of 3 ml/hr, and bladder pressure and accumulated void volume was recorded. For carbachol-induced bladder contractions, carbachol or vehicle was administered intravesically as a 0.1 ml bolus.

In vitro *pharmacology.* Isometric smooth muscle contraction was studied in bladder detrusor strips as described previously (Martin et al., 2000). Briefly, bladders were removed from mice and dissected into Krebs' buffer. Tissues were mounted between two parallel plate electrodes in thermostatically controlled (37°C) organ baths (10 ml) containing Krebs' buffer, gassed continuously with 95% O$_2$ and 5% CO$_2$. The composition of the buffer was (in mM): 118.2 NaCl, 4.6 KCl, 1.6 CaCl$_2$, 1.2 KH$_2$PO$_4$, 1.2 MgSO$_4$, 10 dextrose, 24.8 NaHCO$_3$. The detrusor strips were equilibrated at a resting tension of 0.5 gm for 1 hr with intermittent washing, followed by a KCl (67 mM) prime. KCl-induced contractions were used to normalize the data to control for differences in absolute contractile values resulting from differences in tissue size or health. Changes in isometric force were measured by Grass FTO3c transducers (Grass Instruments, Quincy, MA) and digitized using MacLab data acquisition software (ADInstruments, Colorado Springs, CO). To measure neurogenic-mediated contraction, a train of square electrical pulses was applied for 0.5 sec with pulse frequency increasing in twofold increments (10 V with a pulse width of 0.5 msec). Pulses were delivered by a Grass S88 stimulator and divided across the tissue baths using a MedLab StimuSplitter (Grass Telefactor, West Warwick, RI). Electrically induced contractions were confirmed to be neurogenically mediated by their sensitivity to tetrodotoxin (100 nM). Neurogenic contractions were plotted by fitting a nonlinear equation. In experiments where carbachol was used to induce contraction, cumulative addition of the drug was applied (van Rossum, 1963). The potency of carbachol was determined by fitting mean contractions for each concentration of the drug to the following equation, which is percentage contraction = $[Carbachol]^{nH}/[EC_{50} + (Carbachol)^{nH}]$.

Urethral compliance measurements. Biomechanical study of the mouse urethra was performed as described previously for rats (Jankowski et al., 2004). Female mice were anesthetized with halothane and catheterized (PE-10) through the urethra. The catheter contributed to the maintenance of urethral length after excision of the urethra and bladder. Specimens were mounted on an *ex vivo* testing system (37°C; 95% O$_2$, 5% CO$_2$). Briefly, the system consisted of a hydrostatic reservoir attached to a graduated ring stand for controlled application of intralumenal pressure (measured via a strain gauge pressure transducer connected to a pressure monitor) and a laser micrometer for accurate measurement of outer diameter. Pressure and diameter data were continuously recorded via analog-to-digital conversion to a personal computer. Urethral specimens were preconditioned from 0 to 6 mmHg (each pressure held for 10 sec for 10 cycles), followed by pressure increments of 2 mmHg up to 20 mmHg. The experiment was repeated in random order for three positions along the length of the urethra: proximal (a distance of 30% *in vivo* length from proximal end), middle (50% *in vivo* length from proximal end), and distal (70% *in vivo* length from proximal end). Using the pressure and diameter data recorded, compliance (C) and β stiffness (β) values were calculated for each position:

$$C = \frac{(D_{max} - D_{min})/D_{min}}{(P_{max} - P_{min})},$$

$$\beta = \frac{ln\left(\dfrac{P}{P_s}\right)}{\left(\dfrac{D}{D_s} - 1\right)}.$$

Compliance is a measure of the distensibility of the tissue and provided the relative change in diameter per unit change in pressure. P_{max} and P_{min} represent the maximum and minimum pressures over the pressure range of interest, and D_{max} and D_{min} are the respective diameters measured at these pressures. β stiffness is a parameter that has been widely used to quantify the nonlinear elastic properties of tubular biological tissue. It assumes an exponential relationship of the pressure and diameter, with β being the exponent coefficient. P_s is an arbitrary reference pressure taken here as 10 mmHg, and D_s is the corresponding diameter measured at that pressure. One-way ANOVA was used for statistical analysis with Student–Newman–Keuls *post hoc* testing.

Results

In vitro characterization of the hypersensitive 5-HT$_{3A}$ V13′S mutation in *Xenopus* oocytes

We previously used the *Xenopus* oocyte expression system to characterize homomeric 5-HT$_{3A}$ receptors containing the V13′S mutation in the M2 channel domain (Dang et al., 2000). The mutant receptor showed slower activation and desensitization kinetics (Dang et al., 2000) (Fig. 1*A*) and was ~70-fold more sensitive to serotonin than the wild-type 5-HT$_{3A}$ receptor (5-HT$_{3A}$-WT) (Fig. 1*B*).

In the present study, we performed oocyte expression studies to further characterize 5-HT$_{3A}$ receptors containing the V13′S mutation and to predict the functional properties of homozygous and heterozygous 5-HT$_{3A}$ receptors likely to be expressed in 5-HT$_{3A}$ knock-in mice. Consistent with previous findings, the homomeric V13′S receptor showed higher spontaneous activation in the absence of agonist, manifested as a slightly increased leak current under voltage clamp that is blocked by the channel blocker 8-(*N,N*-diethylamino)-octyl-3,4,5-trimethoxybenzoate (TMB-8; 100 μM) (Dang et al., 2000) (Fig. 1*C*). This spontaneous activity represents <10% of the maximal response. We next assessed heterozygous V13′S/5-HT$_{3A}$-WT pentameric receptors by coinjecting a 1:1 mixture of V13′S and 5-HT$_{3A}$-WT cRNAs into oocytes. The V13′S/5-HT$_{3A}$-WT response waveforms desensitized more slowly than the 5-HT$_{3A}$-WT receptor and were comparable with the V13′S/V13′S waveforms (Fig. 1*A*). The V13′S/5-HT$_{3A}$-WT dose–response relationship was located between the V13′S and 5-HT$_{3A}$-WT, was shallower than either of the former two relationships, appeared to consist of at least two components, and displayed a half-maximal concentration ~10-fold lower than the EC$_{50}$ for the wild-type 5-HT$_{3A}$ receptor (Fig. 1*B*).

While our efforts in generating the 5-HT$_{3A}$ knock-in mice were in progress, the human 5-HT$_{3B}$ subunit cDNA was cloned (Davies et al., 1999), and functional analysis suggested that some native 5-HT$_3$ receptors are heteromultimers containing at least the 5-HT$_{3A}$ and 5-HT$_{3B}$ subunits. The 5-HT$_{3B}$ subunit alone shows no responses to serotonin when expressed in oocytes but modifies serotonin responses when coexpressed with the 5-HT$_{3A}$ subunit. Unexpectedly, when V13′S 5-HT$_{3A}$ and 5-HT$_{3B}$ subunit cRNAs were coinjected into oocytes, the resultant receptor (V13′S/5-HT$_{3B}$) showed high levels of TMB-8-sensitive spontaneous activation (Fig. 1*D*) that was >50% of the maximal response. The waveforms of additional 5-HT$_3$-evoked currents at V13′S/5-HT$_{3B}$ receptors showed more rapid activation and deactivation kinetics than the V13′S/V13′S or V13′S/5-HT$_{3A}$-WT waveforms (Fig. 1*D*). The additional 5-HT$_3$-evoked currents at the V13′S/5-HT$_{3B}$ receptor displayed dose–response relationships with an EC$_{50}$ of ~0.02 nM, resembling those of the V13′S receptor (Fig. 1*E*). The 5-HT$_{3A}$-WT/5-HT$_{3B}$ receptor displayed concentration–response relationships like those of the homomeric 5-HT$_{3A}$-WT receptor, with an EC$_{50}$ of ~2 nM. (Fig. 1*E*). Therefore, the most striking effect of these *in vitro* studies is the
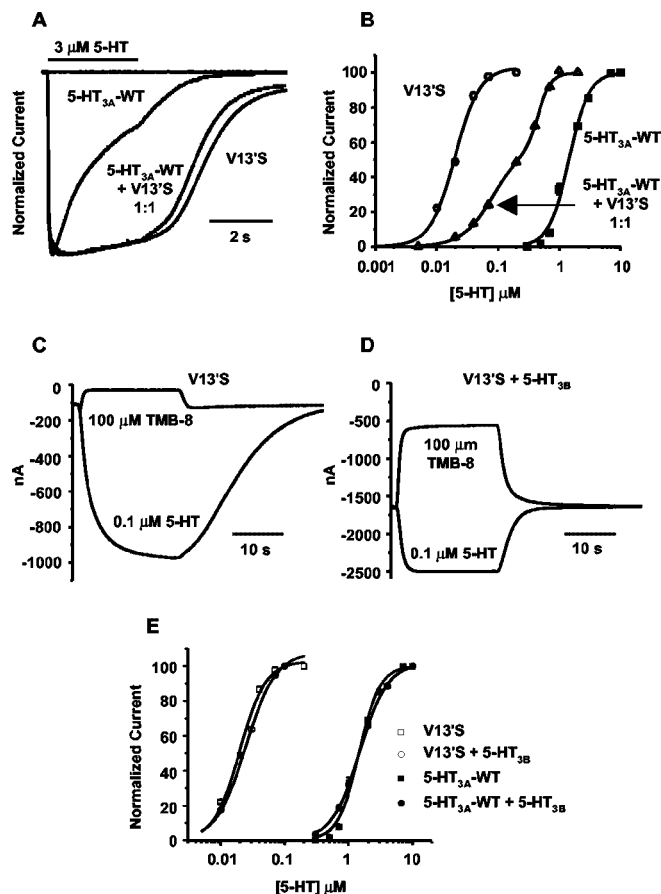

Figure 1. Spontaneous and 5-HT-evoked currents from various combinations of 5-HT$_{3A}$, V13′S, and 5-HT$_{3B}$ receptor subunits expressed in *Xenopus* oocytes. *A*, Representative traces of normalized currents evoked by 3 μM 5-HT at −60 mV. Traces are shown for 5-HT$_{3A}$-WT, V13′S, and a 1:1 mixture of 5-HT$_3$-WT and V13′S cRNAs. The horizontal bar above the traces represents the duration of ligand perfusion through the recording chamber. The flat trace at the baseline level is typical of responses from both the WT and mutant in the presence of 100 nM tropisetron, a 5-HT$_3$ receptor antagonist. *B*, Normalized dose–response relationships of oocytes injected with 5-HT$_{3A}$-WT (solid squares), V13′S (open circles), and a 1:1 mixture of 5-HT$_3$-WT and V13′S (open triangles) cRNAs. *C, D*, Typical voltage-clamp currents from oocytes injected with V13′S cRNA (*C*) or with V13′S plus 5-HT$_{3B}$ cRNA 1:1 (*D*). Holding potential, −60 mV. In each panel, the top trace shows the response to 100 μM TMB-8, and the bottom trace shows the response to 0.1 μM 5-HT. Note the larger leak current at the beginning and end, as well as faster onset and washout to 0.1 μM serotonin in (*D*). The TMB-8-sensitive leak current denotes spontaneous activation of the receptor. *E*, Normalized dose–response relationships of homomultimeric (5-HT$_{3A}$-WT or V13′S only; squares) and heteromultimeric (circles) receptors. Receptors included either the 5-HT$_{3A}$-WT subunit (solid symbols) or V13′S subunit (open symbols).

high level of spontaneous activity in the heteromultimeric V13′S/5-HT$_{3B}$ receptor.

Generation of 5-HT$_{3A}$ receptor knock-in mice

The V13′S valine to serine mutation in the 5-HT$_{3A}$ receptor was introduced into the mouse genome by the targeted exon replacement strategy shown in Figure 2. Heterozygous 5-HT$_{3A}$$^{vs/+}$ mice appeared outwardly normal and bred to produce 5-HT$_{3A}$$^{+/+}$, 5-HT$_{3A}$$^{vs/+}$, and 5-HT$_{3A}$$^{vs/vs}$ mice. Mice carrying the homozygous V13′S knock-in mutation were viable and seemed to develop normally to 2 months of age with no adverse clinical signs or altered behavior. However, as shown in Table 1, male homozygous mutant mice, and to a lesser extent homozygous females and heterozygous males and females, died prematurely (Table 1).
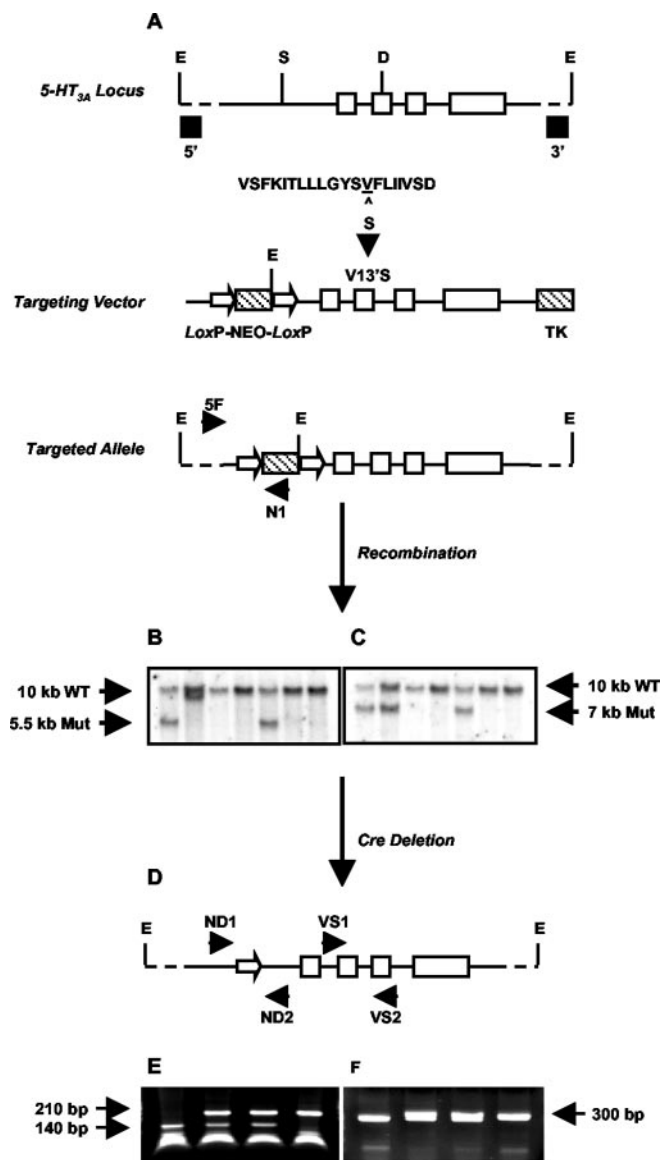
Figure 2. Strategy for generating 5-HT$_{3A}$ knock-in mice through targeted exon replacement. *A*, A 6 kb genomic fragment of the mouse 5-HT$_{3A}$ receptor gene (solid bar) was used to introduce a point mutation (V13'S) into exon (open boxes) 7 coding for the M2 domain of the 5-HT$_{3A}$ receptor. The sequence of the mouse 5-HT$_{3A}$ receptor M2 region (positions 1' to 20') is shown. The Val residue at 13', corresponding to amino acid position 290 in the entire sequence, is underlined. In the 5-HT$_{3A}$ knock-in mouse this is mutated to Ser (S). Neo and TK selection markers (hatched boxes) were inserted into the *Swa*I site (S) in the large intron preceding exon 6 and at the 3' end of the construct, respectively. The Neo sequence was flanked by two *Lox*P sites (open arrowheads). The linearized targeting vector was used for transfection of embryonic stem cells, and the resulting targeted allele was screened as described in Materials and Methods. *B, C,* Representative Southern blots of *Eco*RI (E)-digested genomic DNA were probed with either a 5'-flanking probe (*B*) or a 3'-flanking probe (*C*) to identify the wild-type and mutant (Mut) alleles. *D*, 5-HT$_{3A}$-targeted mice were crossed to Cre-expressing transgenic mice as described in Materials and Methods, resulting in a Neo deleted mutant allele with one 34 bp *Lox*P site remaining in intron 5. *E, F,* Representative PCR screening of genomic DNA from Neo-deleted mice. *E,* Screening across the mutation site using primers VS1 and VS2 followed by *Dde*I (D) digestion. *F,* Screening across the single *Lox*P site after removal of the Neo cassette, using primers ND1 and ND2.

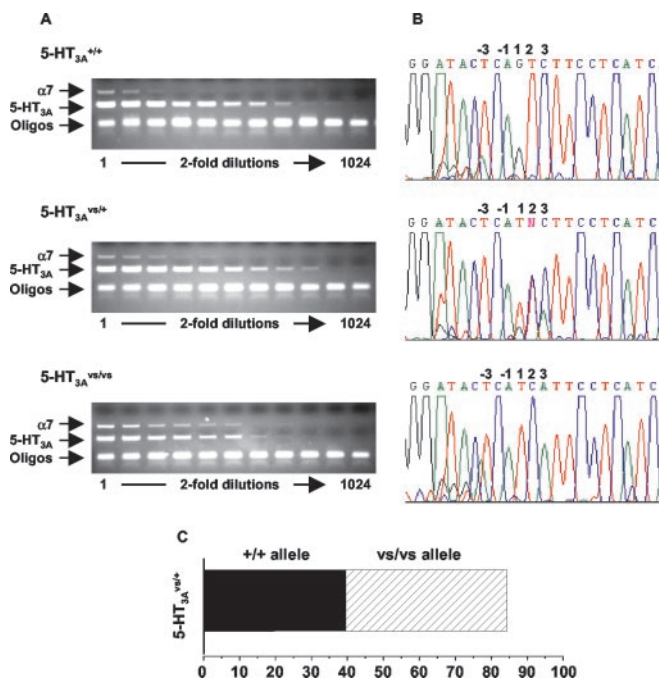## Lowered expression of the 5-HT$_{3A}$ receptor mRNA in 5-HT$_{3A}$$^{vs/vs}$ mice

Introduction of the V13'S mutant receptor into mice would be expected to produce changes in 5-HT$_{3A}$ receptor function consistent with oocyte expression studies but not to alter mRNA

Table 1. Mortality and mean lifespan of 5-HT$_{3A}$ wild-type and mutant mice

| 5-HT$_{3A}$	Sex	Mortality (dead/total)	Mean lifespan of dead (d)
+/+	Male	0/34 (0%)[a]	NA
vs/+	Male	42/144 (29%)	185 ± 11
vs/vs	Male	33/37 (89%)	71 ± 5
+/+	Female	0/43 (0%)[a]	NA
vs/+	Female	15/113 (13%)	209 ± 24
vs/vs	Female	8/43 (19%)	137 ± 23

NA, Not applicable.
[a]Observations made over a period of ∼400 d.

Figure 3. RT-PCR analysis of 5-HT$_{3A}$ mRNA levels in mutant and wild-type mice. *A*, Diminished 5-HT$_{3A}$ mRNA levels in the 5-HT$_{3A}$$^{vs/vs}$ mice. Total RNA was isolated from the SCG of 5-HT$_{3A}$$^{+/+}$, 5-HT$_{3A}$$^{vs/+}$, and 5-HT$_{3A}$$^{vs/vs}$ mice as described in Materials and Methods. Serial dilutions were prepared as indicated, and 1 μl of RNA was used as template for RT-PCR analysis using primers specific for the 5-HT$_{3A}$ receptor (amplicon of ∼300 bp) and the α7 nACh receptor (amplicon of ∼700 bp) as an internal control. Assuming that α7 nACh receptor mRNA did not change, 5-HT$_{3A}$ mRNA was compared with α7 nAChR mRNA at the lowest dilution where signals could be detected. *B*, 5-HT$_{3A}$$^{vs/+}$ mice express comparable levels of the 5-HT$_{3A}$ mutant and wild-type mRNA. RT-PCR sequencing (*B*) of the products shown in *A* were used to estimate the relative abundance of wild-type and mutant mRNA in 5-HT$_{3A}$$^{vs/+}$ mice as described in Materials and Methods. The relative abundance of wild-type (solid bars) and mutant (hashed bars) sequences in the RT-PCR products from 5-HT$_{3A}$$^{vs/+}$ mice was determined by comparing the representation of the pure alleles, and the averaged percentage of the products is shown in the bar graph in *C*. Oligo, Oligonucleotide.

expression from the V13'S mutant allele. To address this directly, we measured 5-HT$_{3A}$ mRNA expression by RT-PCR using serial dilutions of total SCG RNA and primers VS1/VS2 for 5-HT$_{3A}$ receptor mRNA and primers α7-1/α7-2 for α7 nACh receptor mRNA as an internal control (Fig. 3*A*). RT-PCRs from 5-HT$_{3A}$$^{vs/vs}$ mice had more RNA loading than those from 5-HT$_{3A}$$^{+/+}$ and 5-HT$_{3A}$$^{vs/+}$ mice as judged by the relative intensities of the α7 band (Fig. 3*A*). Despite these RNA loading differences, 5-HT$_{3A}$ mRNA signals from 5-HT$_{3A}$$^{+/+}$ and 5-HT$_{3A}$$^{vs/+}$ mice showed little difference, whereas in 5-HT$_{3A}$$^{vs/vs}$ mice, the 5-HT$_{3A}$ bands were substantially less intense (<25%) compared with those seen in the other two genotypes.

Reduced expression of 5-HT$_{3A}$ mRNA in homozygous mu-
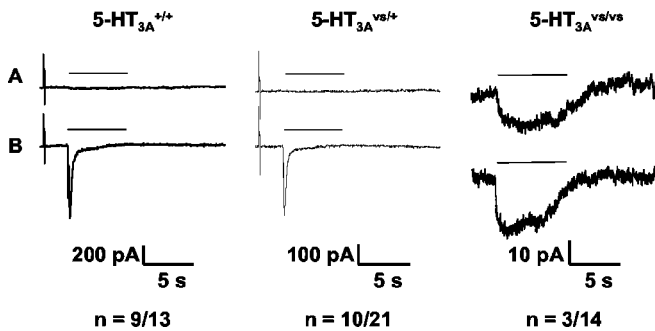
Figure 4. Serotonin-induced whole-cell currents from SCG neurons of 5-HT$_{3A}$$^{+/+}$, 5-HT$_{3A}$$^{vs/+}$, and 5-HT$_{3A}$$^{vs/vs}$ mice. Whole-cell patch-clamp recordings were obtained from primary cultures of SCG neurons. Representative voltage-clamped current responses from 5-HT$_{3A}$$^{+/+}$ (left panel), 5-HT$_{3A}$$^{vs/+}$ (middle panel), and 5-HT$_{3A}$$^{vs/vs}$ (right panel) mice to low (*A*) and high (*B*) concentrations of serotonin are shown. The low concentration of serotonin for 5-HT$_{3A}$$^{+/+}$ and 5-HT$_{3A}$$^{vs/+}$ SCG neurons was 0.3 μM, and that for 5-HT$_{3A}$$^{vs/vs}$ neurons was 0.1 μM, whereas the high concentration was 10 μM in all three. The number of 5-HT$_{3A}$ receptors positive over successfully patched neurons for each genotype is shown below each panel.

tant mice could result from a functional downregulation of constitutively active mutant receptor in all 5-HT$_{3A}$-expressing neurons, or as a consequence of cell death where the only surviving neurons are those expressing low levels of the constitutively activated receptor (Orr-Urtreger et al., 2000). Alternatively, decreased levels of 5-HT$_{3A}$ mRNA could be attributable to selective silencing of the mutant allele because of residual effects of the 34 bp *Lox*P site remaining in intron 5. To test the latter possibility, we measured mRNA expression from the mutant and wild-type alleles by estimating the relative representation of mutant and wild-type sequences obtained by sequencing the RT-PCR products derived from heterozygous 5-HT$_{3A}$$^{vs/+}$ mice (Fig. 3*A,B*) (see Materials and Methods). 5-HT$_{3A}$$^{vs/+}$ mice would be expected to express both alleles in an unbiased manner and showed only minor pathology compared with 5-HT$_{3A}$$^{vs/vs}$ littermates (described below). The RT-PCR sequences shown in Figure 3*B* were used to determine the area under the wild-type and mutant peaks as described in Materials and Methods, and these signals were used to estimate the amount of wild-type and mutant sequence in SCG mRNA from 5-HT$_{3A}$$^{vs/+}$ mice. The analysis gave average estimates of 40% wild-type and 45% mutant sequences in SCG RNA (Fig. 3*C*), suggesting that the mutant allele is expressed at nearly equivalent levels to the wild-type allele in heterozygous 5-HT$_{3A}$$^{vs/+}$ mice.

Lowered functional expression of the 5-HT$_{3A}$ receptor in 5-HT$_{3A}$$^{vs/vs}$ mice
To examine the functional expression of 5-HT$_{3A}$ receptors, we performed whole-cell patch-clamp analysis on SCG neurons isolated from 5-HT$_{3A}$ mutant and wild-type mice (Fig. 4, representative traces shown for each genotype). SCG neurons from 5-HT$_{3A}$$^{+/+}$ and 5-HT$_{3A}$$^{vs/+}$ mice responded to 10 μM 5-HT with rapidly desensitizing currents that varied between 50 and 400 pA among individual neurons at a test potential of −80 mV (Fig. 4*B*, left and middle panels, respectively). The proportion of 5-HT responsive cells was slightly lower in 5-HT$_{3A}$$^{vs/+}$ (10 of 21; 47%) versus 5-HT$_{3A}$$^{+/+}$ (9 of 13; 69%) derived neurons. In contrast, very few neurons from the 5-HT$_{3A}$$^{vs/vs}$ mice responded to 5-HT (3 of 14; 21%), and the few neurons that responded generated only a 15 pA current to 10 μM 5-HT (Fig. 4*B*, right panel). However, the 5-HT$_{3A}$$^{vs/vs}$ neurons showed nondesensitizing currents, and responses to 0.1 μM 5-HT (Fig. 4*A*, right panel) were ~70%

of those seen at 10 μM (Fig. 4*B*, right panel). In contrast, 5-HT at 0.3 μM failed to activate currents in 5-HT$_{3A}$$^{+/+}$ or 5-HT$_{3A}$$^{vs/+}$ SCG neurons (Fig. 4*A*, left and middle panels, respectively). The small responses seen in 5-HT$_{3A}$$^{vs/vs}$ neurons displayed both concentration dependence and kinetic characteristics predicted from oocyte expression studies (Fig. 1) and confirm that the 5-HT$_{3A}$ V13′S receptor expressed *in vivo* is hypersensitive to 5-HT.

Decreased lifespan in 5-HT$_{3A}$$^{vs/vs}$ mice resulting from lower urinary tract dysfunction: pathological evidence
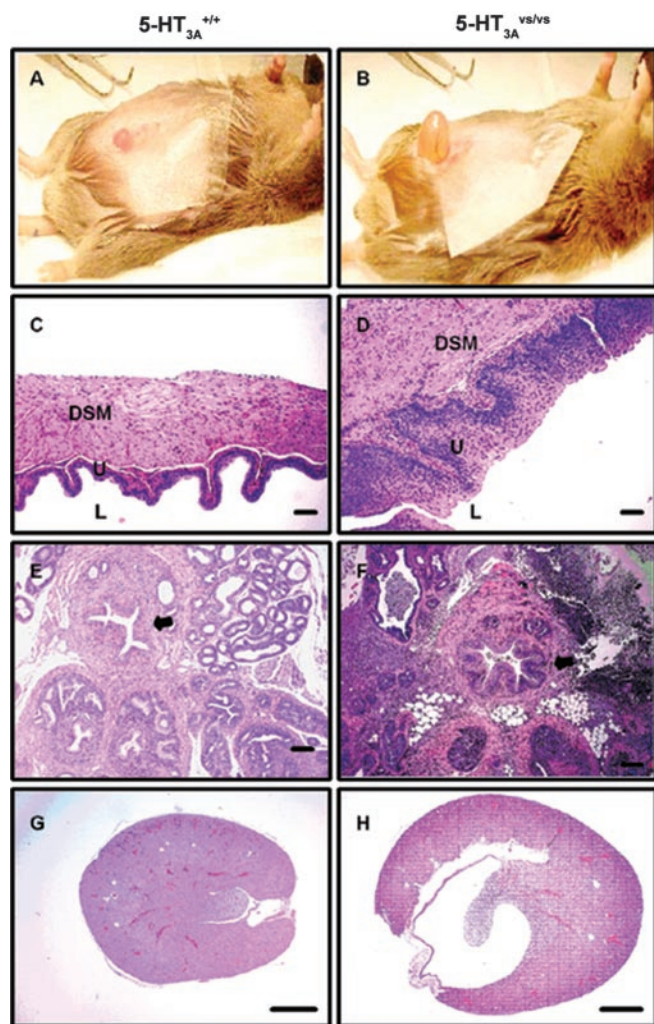Male homozygous mutant mice died at 2–3 months of age (Table 1). Female homozygous mutant mice, followed by male and female heterozygous mice, also had a decreased lifespan compared with 5-HT$_{3A}$$^{+/+}$ mice (Table 1). Moribund 5-HT$_{3A}$ mutant mice were cachectic and had elevated blood urea nitrogen and proteinuria. Renal pelvic dilation resulting from urinary tract obstruction and urinary tract bacterial infections was present, as well as pyelonephritis and tuberulointerstitial nephritis (Fig. 5, compare *H* and *G*). This was likely the main cause of death in 5-HT$_{3A}$$^{vs/vs}$ mice. Both male and female 5-HT$_{3A}$$^{vs/vs}$ mice had hyperdistended urinary bladders characterized by epithelial and detrusor smooth muscle hyperplasia and hypertrophy (Fig. 5, compare *B* and *D* with *A* and *C*). Urinary bladder hypertrophy was evident by 6 weeks of age in male and female 5-HT$_{3A}$$^{vs/vs}$ mice, with significant increases in urinary bladder weight and twofold to threefold increases in urinary bladder to body weight ratios (Table 2). In addition to changes in the urinary bladder, male 5-HT$_{3A}$$^{vs/vs}$ mice also had hyperplasia of prostatic urethral epithelium and surrounding smooth muscle (Fig. 5*F*) and extensive suppurative glandular and periglandular inflammatory cell infiltrate of the prostate and seminal vesicles (Fig. 5, compare *F* and *E*). Proteinaceous plugs were often found in the bladder neck and proximal urethra of 5-HT$_{3A}$$^{vs/vs}$ males. In some mutant mice, we also observed bone marrow hyperplasia and generalized lymphoid atrophy, likely attributed to systemic stress and bacterial infection.

Pathophysiology associated with lower urinary tract organs in 5-HT$_{3A}$$^{vs/vs}$ mice
Urodynamic studies were performed on 5-HT$_{3A}$$^{+/+}$, 5-HT$_{3A}$$^{vs/+}$, and 5-HT$_{3A}$$^{vs/vs}$ mice to determine how histopathological changes observed in 5-HT$_{3A}$ mutant mice influenced urinary bladder function. Figure 6 shows representative filling cystometrograms from conscious mouse cystometry studies in which voiding reflexes were measured in response to a continuous intravesical infusion of saline. In contrast to 5-HT$_{3A}$$^{+/+}$ mice, where normal micturition contractions were observed (Fig. 6, top panel; Table 3), 5-HT3$^{vs/vs}$ mice did not generate voiding contractions (Fig. 6, bottom panel; Table 3). All 5-HT$_{3A}$$^{vs/vs}$ mice studied had a consistent phenotype of overflow incontinence that manifested itself as constant urine dribbling (Fig. 6; Table 3, c.d.). Heterozygous mice had an intermediate phenotype that ranged from decreased void intervals and void volumes to dribbling incontinence (Table 3). Similar cystometric and histopathologic changes were present in both 8- and 12-week-old mice. In separate experiments where natural voiding behavior was measured in metabolic chambers, 5-HT$_{3A}$$^{vs/vs}$ mice also had a phenotype of constant dribbling and lacked normal voids compared with 5-HT$_{3A}$$^{+/+}$ littermate controls (data not shown).

To determine whether detrusor smooth muscle responses were altered in 5-HT$_{3A}$ mutant mice, we measured neurogenic contraction of bladder strips from 6-, 8-, and 12-week-old mice (Fig. 7). Electrical field stimulation of detrusor strips from

Figure 5. *A–H*, Histopathology of the lower urinary tract from 5-HT$_{3A}$$^{+/+}$ (*A, C, E, G*) and 5-HT$_{3A}$$^{vs/vs}$ (*B, D, F, H*) mice. *A, B*, Representative photograph of the hyperdistended urinary bladders seen in 5-HT$_{3A}$$^{vs/vs}$ (*B*) compared with 5-HT$_{3A}$$^{+/+}$ (*A*) mice. *C, D,* H and E stained sections of the urinary bladder wall highlighting the lumen (L), urothelial mucosal layer (U), and the detrusor smooth muscle layer (DSM). *E, F,* H and E stained sections of the prostatic urethra and surrounding prostatic tissue. Note the increased thickness of the urinary bladder wall (*D* vs *C*) and prostatic urethra (arrow in *F* vs *E*) in 5-HT$_{3A}$$^{vs/vs}$ compared with 5-HT$_{3A}$$^{+/+}$ mice, with associated mucosal hyperplasia and smooth muscle hypertrophy. In addition, extensive glandular and periglandular inflammatory cell infiltrate can be seen in the prostatic sections of male 5-HT$_{3A}$$^{vs/vs}$ mice (*F*). *G, H,* Longitudinal sections of kidney from 5-HT$_{3A}$$^{+/+}$ (*G*) and 5-HT$_{3A}$$^{vs/vs}$ (*H*) mice showing the markedly distended renal pelvis in 5-HT$_{3A}$ mutant mice as a consequence of chronic lower urinary tract obstruction. Scale bars: *C, D,* 50 μm; *E–H,* 100 μm.

5-HT$_{3A}$$^{+/+}$ mice induced nerve-mediated contractions that were frequency dependent, whereas bladder strips from 5-HT$_{3A}$$^{vs/+}$ and 5-HT$_{3A}$$^{vs/vs}$ mice failed to produce isometric contractions in response to any frequency of stimulus. The loss of neurogenic-mediated contraction in 5-HT$_{3A}$$^{vs/vs}$ and 5-HT$_{3A}$$^{vs/+}$ mice may have been progressive with age, because weak contractions that were only evident in 6-week-old mice were completely absent at 8 and 12 weeks of age. There were no apparent differences in detrusor contraction between male and female wild-type and mutant mice at 6 weeks of age (Fig. 7*A*). Hence, all remaining *in vitro* bladder studies were performed with tissues from males.

We next determined whether intrinsic properties of the detrusor smooth muscle were also altered by measuring cholinergic-mediated contractions *in vitro* and *in vivo* (Fig. 8). In 8- and 12-week-old 5-HT$_{3A}$ mutant mice, where there was a complete

loss of neurogenic-mediated contraction (Fig. 7), carbachol-induced concentration-dependent contractions of the detrusor smooth muscle in both tissue bath studies *in vitro* (Fig. 8*A,B*) and in conscious cystometry where carbachol was administered intravesically (Fig. 8*C,D*) after establishment of baseline voiding cystometrograms (Fig. 6). No differences were seen in either study between wild-type and mutant mice in terms of the efficacy or potency of carbachol on detrusor smooth muscle responses, except at the two highest doses of carbachol in 12-week-old mice *in vivo*. Together, these data suggest that the V13′S mutation had little or no overall effect on cholinergic receptor function in the urinary bladder.

Decreased nerve fiber density in the urinary bladder urothelium of 5-HT$_{3A}$ knock-in mice

The loss of neurogenic bladder contractions in 5-HT$_{3A}$ mutant mice could be attributable to changes in the neuronal innervation of the urinary bladder. 5-HT$_3$ receptors are found on DRG sensory afferents and on parasympathetic efferents innervating the urinary bladder, and excitotoxic cell death of 5-HT$_{3A}$ V13′S-expressing neurons could lead to a loss of neurons innervating the lower urinary tract. To address this question, we performed whole-mount immunostaining of the bladder urothelium from 5-HT$_{3A}$$^{+/+}$ and 5-HT$_{3A}$$^{vs/vs}$ mice using Substance P immunoreactivity as a marker of primary sensory afferents and PGP 9.5 immunoreactivity as a pan-neuronal marker (Navarro et al., 1997) for all neurons. Consistent with previous observations (Gabella and Davis, 1998), we detected a greater density of nerve fiber innervation in the neck of the urinary bladder compared with the dome in wild-type mice (Fig. 9). In 5-HT$_{3A}$$^{vs/vs}$ mice, staining for both Substance P and PGP 9.5 was markedly decreased compared with that seen in 5-HT$_{3A}$$^{+/+}$ controls. This observation is consistent with the loss of functional responses of the detrusor to nerve-mediated stimulation (Fig. 7) and suggests that a disruption of neuronal networks or connectivity may play a role in the altered lower urinary tract physiology seen in 5-HT$_{3A}$$^{vs/vs}$ mice.

### Assessment of urethral compliance in 5-HT$_{3A}$$^{vs/vs}$ mice

To determine whether changes in urethral tone contributed to the overflow incontinence seen in 5-HT$_{3A}$ mutant mice, we measured the biomechanical properties of urethral compliance and β stiffness. Figure 10 shows low pressure (0–6 mmHg)-induced changes in urethral compliance and β stiffness in 5-HT$_{3A}$$^{+/+}$ and 5-HT$_{3A}$$^{vs/vs}$ mice, demonstrating that no differences were observed in either of these measures. As expected for this system (Jankowski et al., 2004), the proximal urethra was significantly more compliant than the middle and distal portions when subjected to low-pressure stimulations, and this was similar for both 5-HT$_{3A}$$^{+/+}$ and 5-HT$_{3A}$$^{vs/vs}$ mice (Fig. 10*A*). Although differences in β stiffness were not observed between 5-HT$_{3A}$$^{+/+}$ and 5-HT$_{3A}$$^{vs/vs}$ mice for the proximal or middle portions of the urethra, the data did reveal a trend ($p < 0.1$) in which the distal portion of the urethra in 5-HT$_{3A}$$^{vs/vs}$ mice showed less β stiffness compared with wild-type controls over the entire pressure range tested (Fig. 10*B* for 0–6 mmHg) (data not shown).

Discussion

In this study, we demonstrated that a V13′S gain of function mutation in the 5-HT$_{3A}$ receptor subunit resulted in a hypersensitive and constitutively active ion channel, and that expression of this receptor in gene knock-in mice resulted in lower urinary tract dysfunction with overflow incontinence.

Table 2. Urinary bladder and body weights of 5-HT$_{3A}$ wild-type and mutant mice

Age	Sex	5-HT$_{3A}$	Bladder weight (gm)	Body weight (gm)	Bladder/body weight	Fold change[d]
6 weeks	Male	+/+	0.03 ± 0.0	25.65 ± 0.91	1.16×10^{-3}	
	Male	vs/vs	0.04 ± 0.0	24.61 ± 1.12	1.62×10^{-3}	1.4
	Female	+/+	0.02 ± 0.0	17.60 ± 0.23	1.21×10^{-3}	
	Female	vs/vs	0.05 ± 0.0[a]	19.51 ± 1.02	2.41×10^{-3a}	2.0
8 weeks	Male	+/+	0.03 ± 0.0	25.66 ± 0.98	1.33×10^{-3}	
	Male	vs/vs	0.09 ± 0.0[b]	26.07 ± 1.07	3.74×10^{-3c}	2.8
	Female	+/+	0.03 ± 0.0	21.03 ± 0.45	1.27×10^{-3}	
	Female	vs/vs	0.07 ± 0.0[a]	21.44 ± 1.30	3.46×10^{-3a}	2.7

[a]$p < 0.05$.

[b]$p = 0.056$.

[c]$p = 0.062$; unpaired t test comparing 5-HT$_{3A}$$^{+/+}$ and 5-HT$_{3A}$$^{vs/vs}$ mice.

[d]Fold change in bladder/body weight ratios between 5-HT$_{3A}$$^{+/+}$ and 5-HT$_{3A}$$^{vs/vs}$ mice.
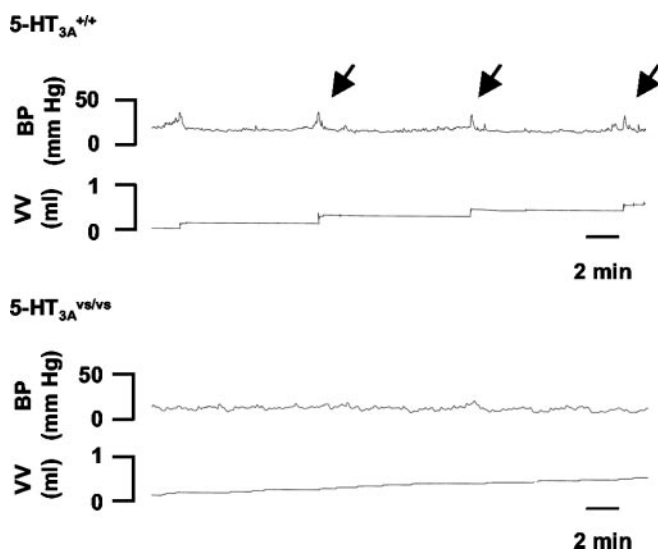
Figure 6. Open-filling cystometry in 5-HT$_{3A}$$^{+/+}$ and 5-HT$_{3A}$$^{vs/vs}$ mice. Representative cystometrograms from conscious 8-week-old male 5-HT$_{3A}$$^{+/+}$ (top panel) and 5-HT$_{3A}$$^{vs/vs}$ (bottom panel) mice. Traces illustrate bladder pressure (BP) recorded in response to a constant infusion of saline and accumulated void volumes (VV) recorded with each micturition. Micturition voiding contractions (arrows) were observed in 5-HT$_{3A}$$^{+/+}$ mice. In contrast, 5-HT$_{3A}$$^{vs/vs}$ mice had a complete loss of micturition contractions, consistent with a phenotype of dribbling overflow incontinence.

Previous studies demonstrated that the V13′S mutation in the A subunit of the 5-HT$_3$ receptor rendered the receptor hypersensitive to 5-HT (Dang et al., 2000). These findings have been extended to show that coexpression of the V13′S 5-HT$_{3A}$ subunit with the wild-type 5-HT$_{3B}$ subunit (Davies et al., 1999) resulted in a constitutively active V13′S/5-HT$_{3B}$ heteromultimeric receptor with 5-HT potency similar to that of the homomeric V13′S receptor. Because 5-HT$_3$ subunits can form homomeric 5-HT$_{3A}$ and heteromeric 5-HT$_{3A/B}$ receptors but not homomeric 5-HT$_{3B}$ receptors (Davies et al., 1999), it is proposed that nearly all functional 5-HT$_3$ receptors in the PNS and CNS of 5-HT$_{3A}$$^{vs/vs}$ mice are hypersensitive to 5-HT and constitutively active. Constitutive activity of a cation-selective excitatory channel could lead to either functional desensitization of the receptor or neuron (as produced by capsaicin on c-fiber sensory afferents), or to persistent neuronal hyperexcitability followed by excitotoxic cell death. In support of the latter hypothesis, SCG neurons from 5-HT$_{3A}$$^{vs/vs}$ mice had decreased levels of 5-HT$_3$ mRNA, showed marked deficits in 5-HT-elicited whole-cell currents, and the few neurons that did respond to 5-HT displayed significant increases in 5-HT potency. Although we have no direct evidence for constitutively active 5-HT$_3$ receptors in neurons of knock-in mice, these data are consistent with the idea that 5-HT$_{3A}$$^{vs/vs}$ mice expressed a gain of function mutation with a high level of constitutive activity, leading to neurotoxic cell death, and low levels of a hypersensitive receptor in the remaining 5-HT$_{3A}$-positive neurons.

Phenotypic characterization of 5-HT$_{3A}$ mutant mice revealed that both males and females developed severe lower urinary tract dysfunction characterized by enlarged urinary bladders with hyperplasia and hypertrophy of the epithelium and detrusor smooth muscle. These bladders showed loss of responsiveness to neurogenic stimulation with little or no change in responsiveness to an exogenous muscarinic agonist, decreased urinary bladder innervation, and a complete loss of micturition contractions with constant urine leakage and overflow incontinence. In addition to changes in the urinary bladder, male 5-HT$_{3A}$$^{vs/vs}$ mice had hyperplasia of prostatic urethral epithelium and surrounding smooth muscle, with inflammatory cell infiltrate of the prostate and seminal vesicles. The main cause of death in 5-HT$_3$ mutant mice was likely urinary tract bacterial infection and renal failure resulting from chronic urinary retention and urinary tract obstruction. 5-HT$_{3A}$$^{vs/vs}$ males died more prematurely than females, suggesting that changes in the prostate and surrounding tissues may have exacerbated a common underlying pathology present in both sexes, possibly by creating a greater degree of outlet obstruction. The effect of the V13′S mutation was also highly penetrant in that heterozygotes showed a loss of responsiveness to neurogenic stimulation and an average lifespan between that of homozygous mutants and wild-type controls. Despite the well described role for 5-HT$_3$ receptors in gastrointestinal, cardiovascular, and CNS functions, we did not observe histopathological changes or overt behavioral signs of dysfunction in these physiological systems in 5-HT$_{3A}$$^{vs/vs}$ mice. Future studies exploring these physiological pathways would be of interest.

Many of the morphological and functional changes in the urinary bladders of 5-HT$_{3A}$$^{vs/vs}$ mice are similar to the changes described for animals or humans with urinary bladder outlet obstruction or neuropathic lesions (Turner and Brading, 1997; Bassuk et al., 2000; Pandita et al., 2000). This raises the question of whether 5-HT$_{3A}$$^{vs/vs}$ mice offer a genetic model for bladder instability associated with partial outlet obstruction or changes in the neuronal control of micturition as seen in neuropathic disease. Partial outlet obstruction in surgically obstructed animals or secondary to BPH is often associated with bladder hypertrophy, detrusor instability, and urinary retention (Hines, 1996; Turner and Brading, 1997). Adaptive changes in the bladder can also occur in response to changes in innervation, and partial denervation of the detrusor has been associated with bladder instability in outflow obstruction, neuropathic disease, and idiopathic

Table 3. Conscious open-filling cystometry parameters in 5-HT$_{3A}$ wild-type and mutant mice

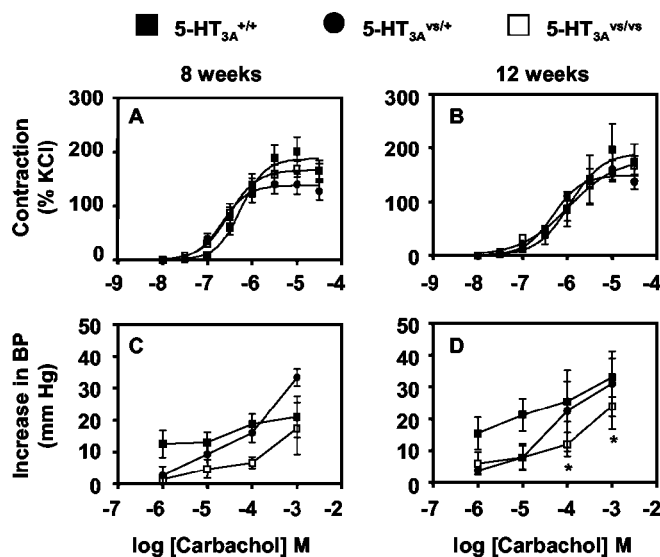| 5-HT$_{3A}$	Sex	Age (weeks)	Void pressure (mmHg)	Void interval (min)	Void volume (ml)	Overflow incontinence[a]
+/+	Male	8	73.3 ± 22.1	8.0 ± 2.6	0.31 ± 0.08	1(4)
vs/+	Male	8	c.d.	c.d.	c.d.	3(3)
vs/vs	Male	8	c.d.	c.d.	c.d.	3(3)
+/+	Female	8	42.7 ± 8.2	10.5 ± 3.4	0.24 ± 0.07	0(4)
vs/+	Female	8	31.0 ± 3.5	6.1 ± 1.1	0.15 ± 0.03	1(4)
vs/vs	Female	8	c.d.	c.d.	c.d.	4(4)
+/+	Male	12	61.0 ± 8.1	5.4 ± 0.5	0.23 ± 0.02	0(6)
vs/+	Male	12	41.7 ± 6.8	7.2 ± 0.4	0.30 ± 0.06	2(5)
vs/vs	Male	12	c.d.	c.d.	c.d.	6(6)
+/+	Female	12	50.7 ± 6.3	6.5 ± 1.4	0.24 ± 0.06	0(6)
vs/+	Female	12	39.7 ± 4.9	4.2 ± 0.5	0.15 ± 0.04	0(3)
vs/vs	Female	12	c.d.	c.d.	c.d.	7(8)

c.d., Constant dribblers.

[a]For each group of mice, the number of overflow incontinent animals is shown against the total number of animals per group (in parentheses).
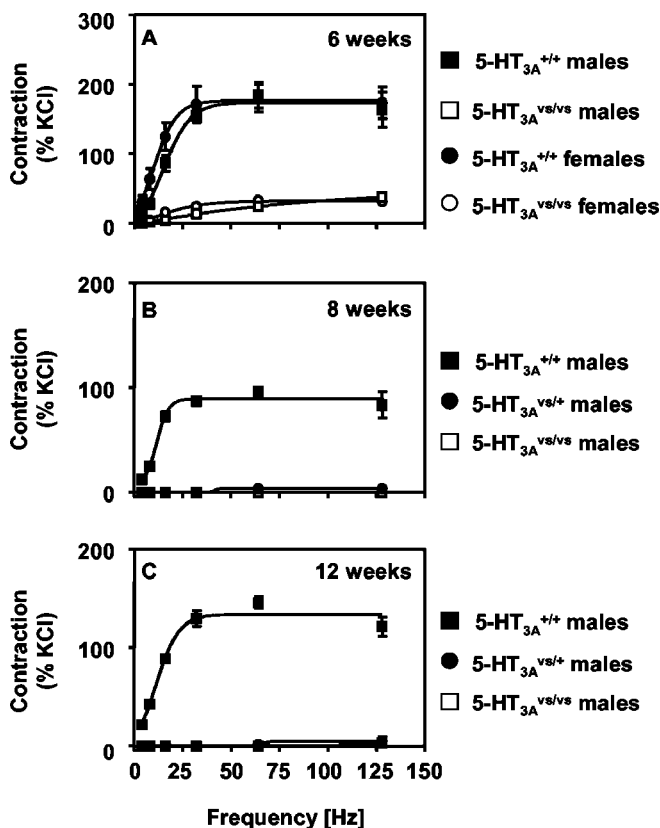
Figure 7. Neurogenic-mediated contractions of detrusor smooth muscle from 5-HT$_{3A}$$^{+/+}$, 5-HT$_{3A}$$^{vs/+}$, and 5-HT$_{3A}$$^{vs/vs}$ mice of various ages. A, Detrusor strips from male and female 6-week-old 5-HT$_{3A}$$^{+/+}$ mice (closed squares and closed circles) responded to electrical field stimulation, whereas bladder strips from male and female 6-week-old 5-HT$_{3A}$$^{vs/vs}$ mice (open squares and open circles) showed minimal responses to neurogenic-mediated contraction. B, C, At 8 (B) and 12 (C) weeks of age, neurogenic-mediated contractions were completely absent in detrusor strips from male 5-HT$_{3A}$$^{vs/+}$ and 5-HT$_{3A}$$^{vs/vs}$ mice (closed circles and open squares), whereas male 5-HT$_{3A}$$^{+/+}$ mice responded to electrical field stimulation (closed squares). Contractile responses were plotted as a percentage of KCl (67 mM)-induced maximal force. Points represent mean contraction ± SEM for n = 3–4 animals per group.

Figure 8. Effect of carbachol on detrusor smooth muscle contraction in male 5-HT$_{3A}$$^{+/+}$, 5-HT$_{3A}$$^{vs/+}$, and 5-HT$_{3A}$$^{vs/vs}$ mice. A, B, Carbachol induced concentration-dependent contractions of bladder smooth muscle *in vitro* in both 8-week-old (A) and 12-week-old (B) 5-HT$_{3A}$$^{+/+}$ (closed squares), 5-HT$_{3A}$$^{vs/+}$ (closed circles), and 5-HT$_{3A}$$^{vs/vs}$ (open squares) mice. C, D, In conscious open filling cystometry, carbachol induced concentration-dependent increases in bladder pressure (BP) in 8-week-old (C) and 12-week-old (D) 5-HT$_{3A}$$^{+/+}$, 5-HT$_{3A}$$^{vs/+}$, and 5-HT$_{3A}$$^{vs/vs}$ mice (symbols as above). In both experiments, no differences were seen in carbachol-induced contractions between wild-type and mutant mice, except at the data points indicated (*). Contraction and bladder pressure changes were plotted as a percentage of KCl (67 mM)-induced maximal force (A, B) and increases from baseline bladder pressure (C, D), respectively. Points represent mean ± SEM for n = 3–6 animals per group. *p < 0.05, statistical significance versus 5-HT$_{3A}$$^{+/+}$ mice.

instability (Turner and Brading, 1997; Lluel et al., 1998; Charlton et al., 1999; Mills et al. 2000; Pandita et al., 2000). Denervation of the detrusor has been most widely associated with loss of post-ganglionic parasympathetic nerves, and it has been suggested that these areas of patchy denervation are responsible for both decreased nerve-evoked contractility and increased excitability contributing to bladder instability (Levin et al., 1995; Turner and
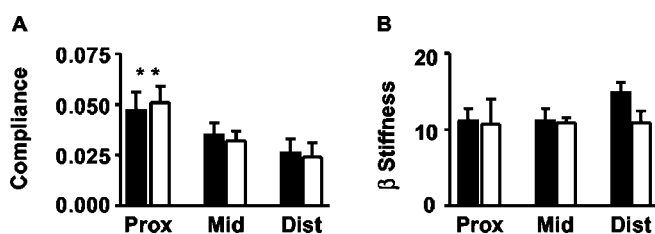
Brading, 1997). Decreased innervation and loss of nerve-evoked bladder contractility, together with bladder hypertrophy and overflow incontinence, is consistent with an outlet obstruction phenotype in 5-HT$_{3A}$$^{vs/vs}$ mice. The current data would suggest that persistent activation of 5-HT$_{3A}$ receptors, and excitotoxic neuronal cell loss, played a principal role in the development of denervation-induced changes in the urinary bladder of these mice.

The localization of 5-HT$_3$ receptors in the dorsal horn of the spinal cord and in peripheral sensory ganglia (Tecott et al., 1993; Johnson and Heinemann, 1995; Kia et al., 1995; Morales and Wang, 2002) suggests that excitotoxic cell death could affect sensory afferent neurons innervating the urinary bladder of 5-HT$_{3A}$$^{vs/vs}$ mice. In the DRG, 5-HT$_3$ receptors are expressed by myelinated Aδ afferents and a small population of unmyelinated
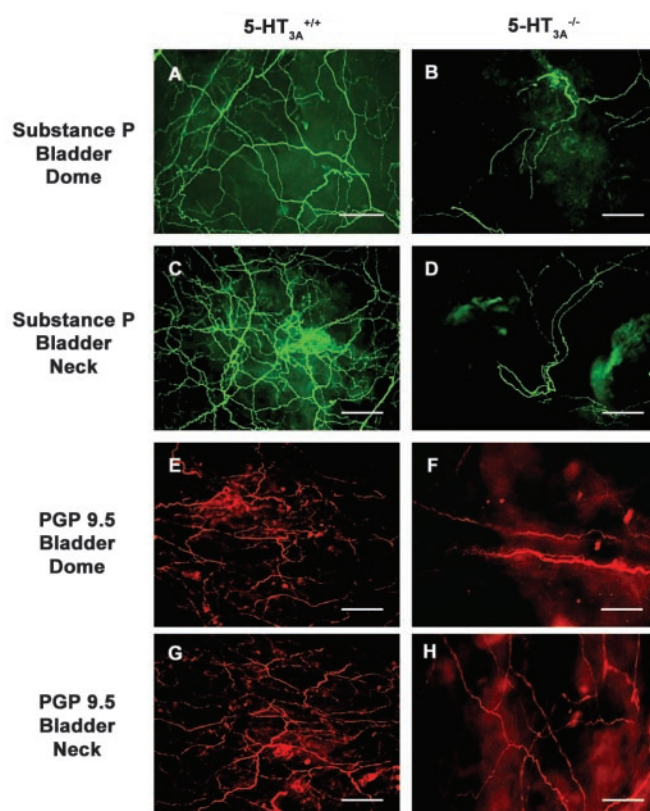
Figure 9. Decreased innervation density in the bladder urothelium of 5-HT$_{3A}$$^{vs/vs}$ mice. A–H, Representative images of whole-mount bladder immunostaining from 8- to 10-week-old 5-HT$_{3A}$$^{+/+}$ (A, C, E, G) and 5-HT$_{3A}$$^{vs/vs}$ (B, D, F, H) mice (n = 3) for Substance P (A–D, green) and PGP 9.5 (E–H, red). Note the decreased density of the fine nerve fibers coursing through the urothelium in both the dome (A, B, E, F) and the neck (C, D, G, H) regions of the urinary bladder. Scale bar: A–H, 50 μm.

Figure 10. Urethral compliance and β-stiffness measurements in female 5-HT$_{3A}$$^{+/+}$ and 5-HT$_{3A}$$^{vs/vs}$ mice. A, B, Data shown represent low pressure (0–6 mmHg)-induced changes in the compliance (A) and β stiffness (B) of the proximal (prox), middle (mid), and distal (dist) urethra in 5-HT$_{3A}$$^{+/+}$ (closed bars) and 5-HT$_{3A}$$^{vs/vs}$ (open bars) mice. Data represent the mean ± SEM for n = 4–5 animals per group. **$p < 0.01$, statistically significant difference in the compliance of the proximal urethra compared with the middle and distal portions in both 5-HT$_{3A}$$^{+/+}$ and 5-HT$_{3A}$$^{vs/vs}$ mice.

C-fibers, which overlap with traditional peptidergic and nonpeptidergic subpopulations (Zeitz et al., 2002). Persistent activation and partial ablation of primary sensory afferents is consistent with the decreased density of Substance P immunoreactive nerve fibers in the bladders of 5-HT$_{3A}$$^{vs/vs}$ mice. Aδ and C-fiber afferents are important in reflex-voiding pathways in the urinary bladder (Yoshimura and de Groat, 1997), and the loss of 5-HT$_{3A}$-expressing afferents could lead to decreased urinary bladder reflexes and compensatory bladder hypertrophy. 5-HT$_3$ receptors are also expressed on many spinal cord neurons, and these receptors have been shown to modulate primary afferent transmission. Spinal 5-HT$_3$ receptors can either facilitate or inhibit nociceptive

processing, the latter via activation of GABAergic inhibitory interneurons (Alhaider et al., 1991; Zeitz et al., 2002). Thus, the loss of 5-HT$_3$-expressing neurons in the CNS might indirectly influence afferent input to the urinary bladder.

5-HT receptors on parasympathetic efferent nerves also modulate detrusor smooth muscle contraction (Barras et al., 1996; Sellers et al., 2000), and evidence supports a role for 5-HT$_3$ receptors in the lower urinary tract. In the rabbit, for example, excitatory effects of 5-HT on the detrusor smooth muscle have been attributed to presynaptic 5-HT$_3$ receptors on parasympathetic efferents (Chen, 1990; Barras et al., 1996). Interestingly, in a rabbit model of BOO, an increased density of ^{3}[H]-5-HT-binding sites was observed in the detrusor smooth muscle (Khan et al., 1999), although the receptor subtype responsible for 5-HT binding was not characterized. Detrusor instability in rabbit BOO models is also associated with partial denervation and cholinergic supersensitivity (Speakman et al., 1987; Rohrmann et al., 1997). It is possible that in 5-HT$_{3A}$ mutant mice, hypersensitive and constitutively active 5-HT$_{3A}$ receptors on parasympathetic nerve fibers innervating the urinary bladder contributed to excitatory responses in the detrusor, with eventual neurotoxic cell death. 5-HT$_{3A}$$^{vs/vs}$ mice did show a slight age-related loss of neurogenic bladder contractions and a decreased density of PGP 9.5 immunoreactive nerve fibers innervating the bladder. This latter observation is consistent with the findings in a recently described model of murine outlet obstruction, where bladder hypertrophy and overactivity were associated with decreased PGP 9.5, nitric oxide synthase, and vesicular ACh transporter immunoreactive nerve terminals in the detrusor smooth muscle (Pandita et al., 2000).

Based on our current data, it remains uncertain whether changes in the urethra contributed to the obstructive pathology seen in 5-HT$_{3A}$$^{vs/vs}$ mice. Although no changes were observed in urethral biomechanical properties between 5-HT$_{3A}$$^{+/+}$ and 5-HT$_{3A}$$^{vs/vs}$ mice, we cannot rule out the possibility of alterations in physiological pathways not measured by this approach, such as the modulation of urethral smooth muscle relaxation by nitric oxide. Constitutive activation of 5-HT$_{3A}$ receptors could also have caused obstruction in other outlet organs such as the bladder neck. Inflammation and hyperplasia of the prostatic urethra in male 5-HT$_3$$^{vs/vs}$ mice was also a probable contributor to bladder outlet obstruction, and this is consistent with the exacerbated disease process observed in male versus female mutant mice.

In summary, our findings suggest a role for 5-HT$_3$ receptors in the development of an outlet obstructive pathology associated with bladder instability and overflow incontinence and provide the first report associating a hypersensitive gain of function mutation in the 5-HT$_3$ receptor with a neuro-urological pathology. The phenotype of this strain contrasts with that of 5-HT$_{3A}$ receptor null mice (Zeitz et al., 2002), which display reduced tissue injury-induced persistent nociception but no obvious urinary tract malfunction. These findings emphasize that complementary information can be obtained from gain of function and loss of function genetic manipulations (Lester et al., 2003). The knock-in approach for studying gain of function mutations has been described previously for nACh receptors, where point mutations in the M2 domain of the α7 (Orr-Urtreger et al., 2000; Broide et al., 2002) and α4 (Labarca et al., 2001) nACh receptor subunits resulted in hypersensitivity to both acetylcholine and nicotine in oocytes in vitro. Similar to 5-HT$_{3A}$$^{vs/vs}$ mice, expression of hypersensitive α4 and α7 nACh receptors in vivo resulted in reduced levels of receptor subunit protein levels, neuronal cell death, and phenotypic behavioral changes (Labarca et al., 2001;

Broide et al., 2002). Interestingly, previous studies have also shown that knock-out mice lacking either the $\alpha3$ subunit or both the $\beta2$ and $\beta4$ subunits of the nACh receptor had profoundly enlarged bladders with overflow incontinence, and developed urinary tract infections and bladder stones (Xu et al., 1999a; Xu et al., 1999b). Taken together, these data may help us to better understand the role of ligand-gated ion channels such as the 5-HT$_3$ and nACh receptors in the neurophysiologic control of the bladder and the lower urinary tract.

References

Alhaider AA, Lei SZ, Wilcox GL (1991) Spinal 5-HT$_3$ receptor mediated antinociception: possible release of GABA. J Neurosci 11:1881–1888.

Barras M, Van der Graaf PH, Angel I (1996) Characterization of the 5-HT receptor potentiating neurotransmission in rabbit bladder. Eur J Pharmacol 318:425–428.

Bassuk JA, Grady R, Mitchell M (2000) The molecular era of bladder research: transgenic mice as experimental tools in the study of outlet obstruction. J Urol 164:170–179.

Broide RS, Salas R, Ji D, Paylor R, Patrick JW, Dani JA, De Biasi M (2002) Increased sensitivity to nicotine-induced seizures in mice expressing the L250T $\alpha7$ nicotinic acetylcholine receptor mutation. Mol Pharmacol 61:695–705.

Charlton RG, Morley AR, Chambers P, Gillespie JI (1999) Focal changes in nerve, muscle and connective tissue in normal and unstable human bladder. BJU International 84:953–960.

Chen HI (1990) Evidence for the presynaptic action of 5-hydroxytryptamine and the involvement of purinergic innervation in the rabbit lower urinary tract. Br J Pharmacol 101:212–216.

Cockayne DA, Hamilton SG, Zhu Q-M, Dunn PM, Zhong Y, Novakovic S, Malmberg AB, Cain G, Berson A, Kassotakis L, Hedley L, Lachnit WG, Burnstock G, McMahon SB, Ford APDW (2000) Urinary bladder hyporeflexia and reduced pain-related behavior in P2X$_3$-deficient mice. Nature 407:1011–1015.

Dang H, England PM, Farivar SS, Dougherty DA, Lester HA (2000) Probing the role of a conserved M1 proline residue in 5-hydroxytryptamine$_3$ receptor gating. Mol Pharmacol 57:1114–1122.

Davies PA, Pistis M, Hanna MC, Peters JA, Lambert JJ, Hales TG, Kirkness EF (1999) The 5-HT$_{3B}$ subunit is a major determinant of serotonin-receptor function. Nature 397:359–363.

Dubin AE, Huvar R, D'Andrea MR, Pyati J, Zhu JY, Joy KC, Wilson SJ, Galindo JE, Glass CA, Luo L, Jackson MR, Lovenberg TW, Erlander MG (1999) The pharmacological and functional characteristics of the serotonin 5-HT$_{3A}$ receptor are specifically modified by a 5-HT$_{3B}$ receptor subunit. J Biol Chem 274:30799–30810.

Eide PK, Hole K (1993) The role of 5-hydroxytryptamine (5-HT) receptor subtypes and plasticity in the 5-HT systems in the regulation of nociceptive sensitivity. Cephalalgia 13:75–85.

Gabella G, Davis C (1998) Distribution of afferent axons in the bladder of rats. J Neurocyto 27:141–155.

Galligan JJ (2002) Ligand-gated ion channels in the enteric nervous system. Neurogastroenterol Motil 14:611–623.

Hamon M, Gallissot MC, Menard F, Gozlan H, Bourgoin S, Verge D (1989) 5-HT3 receptor binding sites are on capsaicin-sensitive fibres in the rat spinal cord. Eur J Pharmacol 164:315–322.

Hines JE (1996) Symptom indices in bladder outlet obstruction. Br J Urol 77:494–501.

Jackson MB, Yakel JL (1995) The 5-HT$_3$ receptor channel. Annu Rev Physiol 57:447–468.

Jankowski RJ, Prantil RL, Fraser MO, Chancellor MB, deGroat WC, Huard J, Vorp DA (2004) Development of an experimental system for the study of urethral biomechanical function. Am J Physiol Renal Physiol 286:F225–F232.

Johnson DS, Heinemann SF (1995) Detection of 5-HT$_3$R-A, a 5-HT$_3$ receptor subunit, in submucosal and myenteric ganglia of rat small intestine using in situ hybridization. Neurosci Lett 184:67–70.

Khan MA, Dashwood MR, Thompson CS, Mumtaz FH, Morgan RJ, Mikhailidis DP (1999) Time-dependent up-regulation of neuronal 5-hydroxytrypta-

mine binding sites in the detrusor of a rabbit model of partial bladder outlet obstruction. World J Urol 17:255–260.

Kia HK, Miquel M-C, McKernan RM, Laporte A-M, Lombard M-C, Bourgoin S, Hamon M, Verge D (1995) Localization of 5-HT3 receptors in the rat spinal cord: immunohistochemistry and in situ hybridization. NeuroReport 6:257–261.

Kidd EJ, Laporte AM, Langlois X, Fattaccini CM, Doyen C, Lombard MC, Gozlan H, Hamon M (1993) 5-HT3 receptors in the rat central nervous system are mainly located on nerve fibres and terminals. Brain Res 612:289–298.

Labarca C, Schwarz J, Deshpande P, Schwarz S, Nowak MW, Fonck C, Nashmi R, Kofuji P, Dang H, Shi W, Fidan M, Khakh BS, Chen Z, Bowers BJ, Boulter J, Wehner JM, Lester HA (2001) Point mutant mice with hypersensitive alpha 4 nicotinic receptors show dopaminergic deficits and increased anxiety. Proc Natl Acad Sci USA 98:2786–2791.

Leslie RA, Reynolds DJ, Andrews PL, Grahame-Smith DG, Davis CJ, Harvey JM (1990) Evidence for presynaptic 5-hydroxytryptamine3 recognition sites on vagal afferent terminals in the brainstem of the ferret. Neuroscience 38:667–673.

Lester H, Fonck C, Tapper A, McKinney S, Damaj M, Balogh S, Owens J, Wehner J, Collins A, Labarca C (2003) Hypersensitive knock-in mouse strains identify receptors and pathways for nicotine action. Curr Opin Drug Dev 6:633–639.

Lester HA, Karschin A (2000) Gain of function mutants: ion channels and G protein-coupled receptors. Annu Rev Neurosci 23:89–125.

Levin RM, Monson FC, Haugaard N, Buttyan R, Hudson A, Roelofs M, Sartone S, Wein AJ (1995) Genetic and cellular characteristics of bladder outlet obstruction. Urol Clin North Am 22:263–283.

Lluel P, Duquenne C, Martin D (1998) Experimental bladder instability following bladder outlet obstruction in the female rat. J Urol 160:2253–2257.

Maricq AV, Peterson AS, Brake AJ, Myers RM, Julius D (1991) Primary structure and functional expression of the 5-HT$_3$ receptor, a serotonin-gated ion channel. Science 254:432–437.

Martin RS, Luong LA, Welsh NJ, Eglen RM, Martin GR, MacLennan SJ (2000) Effects of cannabinoid receptor agonists on neuronally-evoked contractions of urinary bladder tissues isolated from rat, mouse, pig, dog, monkey and human. Br J Pharmacol 129:1707–1715.

Merahi N, Orer HS, Laporte AM, Gozlan H, Hamon M, Laguzzi R (1992) Baroreceptor reflex inhibition induced by the stimulation of serotonin3 receptors in the nucleus tractus solitarius of the rat. Neuroscience 46:91–100.

Mills IW, Greenland JE, McMurray G, McCoy R, Ho KM, Noble JG, Brading AF (2000) Studies of the pathophysiology of idiopathic detrusor instability: the physiological properties of the detrusor smooth muscle and its pattern of innervation. J Urol 163:646–651.

Morales M, Wang SD (2002) Differential composition of 5-hydroxytryptamine$_3$ receptors synthesized in rat CNS and peripheral nervous system. J Neurosci 22:6732–6741.

Navarro X, Verdú E, Wendelschafer G, Kennedy WR (1997) Immunohistochemical study of skin reinnervation by regenerative axons. J Comp Neurol 380:164–174.

Nowak MW, Kearney PC, Sampson JR, Saks ME, Labarca CG, Silverman SK, Zhong W, Thorson J, Abelson JN, Davidson N, Schultz PG, Dougherty DA, Lester HA (1995) Nicotinic receptor binding site probed with unnatural amino acid incorporation in intact cells. Science 268:439–442.

Orr-Urtreger A, Broide RS, Kasten MR, Dang H, Dani JA, Beaudet AL, Patrick JW (2000) Mice homozygous for the L250T mutation in the $\alpha7$ nicotinic acetylcholine receptor show increased neuronal apoptosis and die within 1 day of birth. J Neurochem 74:2154–2166.

Pandita RK, Fujiwara M, Alm P, Andersson K-E (2000) Cystometric evaluation of bladder function in non-anesthetized mice with and without bladder outlet obstruction. J Urol 164:1385–1389.

Rohrmann D, Monson FC, Damaser MS, Levin RM, Duckett JW, Zderic SA (1997) Partial bladder outlet obstruction in the fetal rabbit. J Urol 158:1071–1074.

Sellers DJ, Chess-Williams R, Chapple CR (2000) 5-hydroxytryptamine-induced potentiation of cholinergic responses to electrical field stimulation in pig detrusor muscle. Br J Urol 86:714–718.

Sevoz-Couche C, Comet MA, Hamon M, Laguzzi R (2003) Role of nucleus tractus solitarius 5-HT$_3$ receptors in the defense reaction-induced inhibition of the aortic baroreflex in rats. J Neurophysiol 90:2521–2530.

Speakman MJ, Brading AF, Gilpin CJ, Dixon JS, Gilpin SA, Gosling JA (1987) Bladder outflow obstruction–a cause of denervation supersensitivity. J Urol 138:1461–1466.

Tecott LH, Maricq AV, Julius D (1993) Nervous system distribution of the serotonin 5-HT$_3$ receptor mRNA. Proc Natl Acad Sci USA 90:1430–1434.

Turner WH, Brading AF (1997) Smooth muscle of the bladder in the normal and the diseased state: pathophysiology, diagnosis and treatment. Pharmacol Ther 75:77–110.

van Hooft JA, Yakel JL (2003) 5-HT$_3$ receptors in the CNS: 3B or not 3B. Trends Pharmacol Sci 24:157–160.

van Rossum JM (1963) Cumulative dose-response curves. Arch Int Pharmacodyn 143:299–330.

Veelken R, Hilgers KF, Leonard M, Scrogin K, Ruhe J, Mann JF, Luft FC (1993) A highly selective cardiorenal serotonergic 5-HT$_3$-mediated reflex in rats. Am J Physiol 264:H1871–H1877.

Xu W, Gelber S, Orr-Urtreger A, Armstrong D, Lewis RA, Ou C-N, Patrick J, Role LW, Biasi MD, Beaudet AL (1999a) Megacystis, mydriasis and ion channel defect in mice lacking the α3 neuronal nicotinic acetylcholine receptor. Proc Natl Acad Sci USA 96:5746–5751.

Xu W, Orr-Urtreger A, Nigro F, Gelber S, Sutcliffe CB, Armstrong D, Patrick JW, Role LW, Beaudet AL, Biasi MD (1999b) Multiorgan autonomic dysfunction in mice lacking the β2 and the β4 subunits of neuronal acetylcholine receptors. J Neurosci 19:9298–9305.

Yoshimura N, de Groat WC (1997) Neural control of the lower urinary tract. Br J Urol 4:111–125.

Zeitz KP, Guy N, Malmberg AB, Dirajlal S, Martin WJ, Sun L, Bonhaus DW, Stucky CL, Julius D, Basbaum AI (2002) The 5-HT$_3$ subtype of serotonin receptor contributes to nociceptive processing via a novel subset of myelinated and unmyelinated nociceptors. J Neurosci 22:1010–1019.

Zinyk DL, Mercer EH, Harris E, Anderson DJ, Joyner AL (1998) Fate mapping of the mouse midbrain-hindbrain constriction using a site-specific 3recombination system. Curr Biol 21:665–668.